



# Study of Lorentz invariance violation in polarized top quark decay

Taghi Ebrahimi, S. Mohammad Moosavi Nejad<sup>1</sup>, Zahra Rezaei<sup>a</sup>

Faculty of Physics, Yazd University, P.O. Box 89195-741, Yazd, Iran

Received: 14 October 2024 / Accepted: 9 March 2025  
© The Author(s) 2025

**Abstract** Different processes have yet studied the effect of Lorentz symmetry violation and different limits have determined for the Lorentz violation (LV) coefficients. Top-quark physics offers a rich variety of options for seeking Lorentz-invariant physics beyond the standard model (SM). In this work, we study the effect of Lorentz-violating terms on the partonic decay rates of polarized top quark. The polar and azimuthal correlations between the planes formed by the vectors  $(\vec{p}_l, \vec{p}_{X_b})$  and  $(\vec{p}_l, \vec{P}_t)$  in the semileptonic rest frame decay of a polarized top quark belongs to a class of polarization observables involving the top quark so that the azimuthal correlation vanishes at the Born term level in the SM. We will show that the LV effect leads to different results for the partonic decay rates, specifically the azimuthal correlation contribution deviates from the corresponding SM value. These spin-momentum correlations between the top quark spin and its decay product momenta will allow to search for the non-SM effects. We also determine an upper bound on the LV coefficients within the SME framework as  $c_L^{XZ} \leq 23.6 \times 10^{-3}$  and  $c_L^{XX} \leq 2.65 \times 10^{-3}$  which are compatible with the bounds on LV from the CMS Collaboration, where the LV is introduced as an extension of the SM with an effective field theory predicting the modulation of  $t\bar{t}$  cross section with sidereal time.

## 1 Introduction

In the standard model (SM) of particle physics the Gauge, CPT and Lorentz symmetries have been the main foundation of this model from the beginning. While, the CPT theorem anticipates the equality of some quantities such as the mass, life-time, gyromagnetic ratio and charge-to-mass ratio for particles and corresponding anti-particles, the Lorentz invariance refers to a basic feature of nature that says experimental

observables are independent of the orientation or boost velocity of the laboratory frame through space. Despite of all SM successes, this model does not show a theory of everything because, firstly, it does not include the gravity described by the general relativity and, secondly, does not have convincing answers for the candidates of matter–antimatter asymmetry, dark matter, hierarchy problem, etc. To solve these problems and ambiguities, some new theories or extended models of SM (known as beyond SM theories) have been developed during recent decades. Among all suggested models, a fundamental theory which unifies the gravity and the SM would emerge at energies approaching Planck scale ( $\approx 10^{19}$  GeV). Basically, tiny violations of the CPT and Lorentz symmetries could emerge in the models unifying the gravity theory with quantum mechanics [1,2]. In this context, the Lorentz invariance violation is allowed in string theory, supersymmetry and Horava–Lifshitz gravity [3]. In order to study the Lorentz symmetry violations in the context of quantum field theory (QFT) a new theory has been established by Colladay and Kostelecky [4,5] which is conventionally called as the SM Extension (SME). This idea includes the SM, the General Relativity and all possible operators which break Lorentz symmetry. Basically, the Effective Quantum Field Theories such as the SME introduce the Lorentz symmetry and CPT violations through spontaneous symmetry breaking (SSB) caused by hypothetical background fields. A Lorentz violating term in the SME Lagrange density is an observer scalar density formed by contracting a Lorentz-violating operator with a coefficient for Lorentz violation that controls the size of the associated effects. The SME provides a realistic and calculable framework for analyses of experimental data searching for deviations from Lorentz and CPT invariance [6,7]. This theory is categorized into two sectors: (1) the minimal SME (a renormalizable theory in Minkowski space-time) containing the operators with the mass dimensions  $d \leq 4$  which keeps conventional quantization, gauge invariance, hermiticity, power counting renor-

<sup>a</sup> e-mail: [zahra.rezaei@yazd.ac.ir](mailto:zahra.rezaei@yazd.ac.ir) (corresponding author)

malizability and positivity of energy, and (2) the nonminimal version which does also include operators of higher dimensions. The structure of SME is one way to study the Lorentz violation (LV) so that an alternative procedure is to modify just the SME interactions part via nonminimal couplings. In fact, through this approach a nonminimal coupling term is added to the covariant derivative which may be CPT-odd or CPT-even. This leads to, for example, the improved photon-fermion vertices in QED. In Ref. [8], authors have studied the Lorentz violation in hadron production process from pair annihilation induced by a nonminimal coupling and in Ref. [9] this possibility has been applied to specify the LV bounds on Bhabha scattering process. In Ref. [10] the same approach has been employed for studying the spectrum of hydrogen atom. Simultaneously with the theoretical progresses, many experimental checks on LV improvements have also been done so that several constraints on LV parameters have been determined, e.g. clock-comparison experiments [11], hyperfine structure of muonium ground state [12], hyperfine spectroscopy of hydrogen and anti-hydrogen [13], etc., see also Refs. [14–17]. Among them, the clock anisotropy [18] which is a spectroscopic experiment is one of the most exact experiments where the LV parameters are defined as in the SME theory. It should be noted that, the SME contains a number of possible terms which violate local Lorentz symmetry by coupling to particles spin [11]. In the present work, we probe the prospects for studying the foundational Lorentz and CPT symmetries of the SM in the polarized top quark decay and try to determine an upper limit on the LV coefficients in the minimal SME framework. Note that, choosing a reference frame is needed to report the measurements of LV coefficients. A conventional choice is the sun-centered frame (SCF) which can be considered as inertial in the lifetime of a physics experiment. In Sect. 5, we will describe the sun-centered frame and its relation with the top rest frame through the transformation matrices.

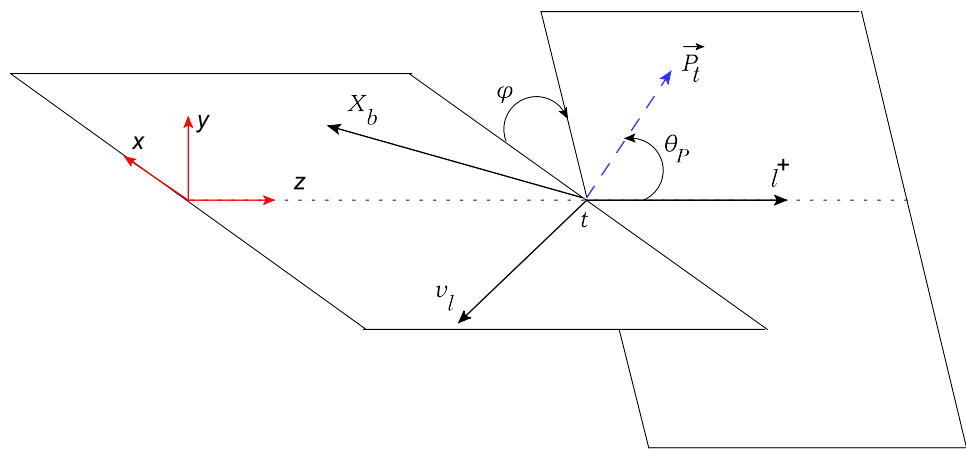
The discovery of top quark in 1995 at the Fermilab Tevatron [19] opened a new era for studying the SM of particle physics. The CERN-LHC is known as a superlative top factory by producing several million single-top or single-antitop events and even more top-antitop pairs over the next few years. This volume of data both allows to carry out precise measurements of the top quark properties and search for new physics from models constructed within a conventional field theoretic context. Some theoretical motivations for top quark studies arise from the notion that Lorentz symmetry violation in a complete space-time theory involving gravity is expected to be spontaneous rather than explicit, as the latter is generically incompatible with conventional Riemann geometry or technically unnatural [20, 21]. In the SM, top quark has a very short lifetime ( $\approx 0.5 \times 10^{-24}$  s [22]) so it decays rapidly before hadronization takes place. Due to the Cabibbo–Kobayashi–Maskawa (CKM) mixing

matrix element  $|V_{tb}| \approx 1$  [23, 24], at the lowest order the top quark decay width is almost exclusively dominated by  $t \rightarrow b W^+ \rightarrow b l^+ \nu_l$ . Since the top quark life time is much shorter than the typical time required for the QCD interactions to randomize its spin, thus its full polarization content is preserved and passes on to its decay products. Hence, the top quark polarization reveals itself in the angular decay distribution and can be studied through the angular correlations between the direction of top quark spin and the momenta of decay products. Through this work, we analyze the angular correlation in a helicity coordinate system where the event plane, including the top and its decay products, is defined in the  $(\hat{X}, \hat{Z})$  plane with the  $\hat{Z}$ -axes along the lepton momentum (see Fig. 1). In this frame, the polarization vector of top quark ( $\vec{P}_t$ ) is evaluated with respect to the direction of lepton momentum ( $\vec{p}_l$ ). Basically, to define the planes we need to measure the momentum directions of the momenta  $\vec{p}_{X_b}$  and  $\vec{p}_l$  and the polarization direction of top quark, where the evaluation of momentum direction of  $\vec{p}_{X_b}$  requires the use of a jet finding algorithm. The spin direction of top quark must be obtained from theoretical input. For example, in  $e^+e^-$  annihilation the polarization degree of the top quark can be tuned with the help of polarized beams [25], so that a polarized linear  $e^+e^-$  Collider could be considered as a copious source of close to zero and close to 100% polarized top quarks.

The azimuthal correlations between the event plane and the intersecting ones to this plane belong to a class of polarization observables involving the top quark in which the leading-order (LO) contribution gives a zero result in the SM, so that the non-zero contributions can arise from higher order radiative corrections. Our analytical results in the minimal SME theory show that the breaking of Lorentz symmetry leads to a non-zero value for this correlation and also the unusual dependence of the unpolarized, polar and azimuthal differential rates on the orientation of the scattering plane in the center-of-mass (COM) frame. Although, the azimuthal decay rate in the SME theory is small, but since highly polarized top quarks with more accuracy will become available at higher luminosity hadron colliders through single top production processes [26], it may then be feasible to experimentally measure the azimuthal correlations produced through top decays.

This paper is structured as follows. In Sect. 2, we introduce the angular rate structure by describing the technical details of our calculations. In Sect. 3, the minimal SME theory is described in detail. Our analytic results to the angular distributions of partial decay rates in the SME theory are presented in Sect. 4. Section 5 is devoted to introduce the sun-centered frame (SCF). In Sect. 6, our numerical analysis is presented and discussed. In Sect. 7 the summary and conclusions are given.

**Fig. 1** The azimuthal ( $\phi$ ) and polar ( $\theta_P$ ) angles in the rest frame decay of a polarized top quark.  $\vec{P}_t$  stands for the polarization vector of the top quark and the event plane defines the ( $X - Z$ ) plane



## 2 Angular structure of partial decay rate

In the current-induced  $t \rightarrow b$  transition, the dynamics of process is embodied in the hadron tensor  $H^{\mu\nu} \propto \sum_X \langle t | J^{\mu\dagger} | X \rangle \langle X | J^\nu | t \rangle$ , where the SM current combination is given by  $J_\mu = J_\mu^V - J_\mu^A$ . Here, the left-chiral components of the weak current are given by the vector and axial-vector contributions:  $J_\mu^V \propto \bar{\psi}_b \gamma_\mu \psi_t$  and  $J_\mu^A \propto \bar{\psi}_b \gamma_\mu \gamma_5 \psi_t$ . The general angular distribution of the differential decay width  $d\Gamma/dx$  of a polarized top quark decaying into a charged lepton  $l^+$  and a neutrino  $\nu_l$  and a jet  $X_b$  (with bottom quantum numbers) is expressed as [27,28]

$$\begin{aligned} & \frac{d^3\Gamma}{dx_l d\cos\theta_P d\phi} (t(\uparrow) \rightarrow b l^+ \nu_l) \\ &= \frac{1}{4\pi} \left\{ \frac{d\Gamma_A}{dx_l} + P \frac{d\Gamma_B}{dx_l} \cos\theta_P + P \frac{d\Gamma_C}{dx_l} \sin\theta_P \cos\phi \right\}, \end{aligned} \quad (1)$$

where, the scaled energy fraction of lepton is defined as  $x_l = 2p_l \cdot p_t / m_t^2$  that in the top rest frame is simplified as:  $x_l = 2E_l/m_t$  ( $y^2 \leq x_l \leq 1$ ). In the equation above, the polar ( $\theta_P$ ) and azimuthal ( $\phi$ ) angles show the orientation of the plane including the spin of top quark relative to the event plane (Fig. 1) and  $P$  is the magnitude of top quark polarization so that  $P = 0$  stands for an unpolarized top quark while  $P = 1$  corresponds to 100% top quark polarization. In the notation above,  $d\Gamma_A/dx_l$  corresponds to the unpolarized differential decay width while  $d\Gamma_B/dx_l$  and  $d\Gamma_C/dx_l$  describe the polar and azimuthal correlations between the polarization of top quark and its decay products, respectively. The NLO radiative corrections to the unpolarized rate  $\Gamma_A$ , the polar correlation function  $\Gamma_B$  and the azimuthal correlation function  $\Gamma_C$  have been studied extensively before. The Born term contribution to the azimuthal correlation  $\Gamma_C$  vanishes which is a consequence of the left-chiral (V-A)(V-A) nature of the current-current interaction in the SM.

### 2.1 Analytic results for the angular distributions of the differential decay width: Born-level

For the process  $t(\uparrow, p_t) \rightarrow b(p_b) + W^+(p_W) \rightarrow b(p_b) l^+(p_l) \nu_l(p_\nu)$ , it is straightforward to evaluate the Born term contribution to its decay rate. Through the Breit–Wigner prescription [29], the Born amplitude is written as

$$\begin{aligned} M^{LO} = & \bar{u}(p_b, s_b) \left( -\frac{i g_W |V_{tb}|}{2\sqrt{2}} \gamma_\mu (1 - \gamma_5) \right) u(p_t, s_t) \\ & \times \left[ \frac{-i(g^{\mu\nu} - \frac{p_W^\mu p_W^\nu}{m_W^2})}{p_W^2 - m_W^2 + i m_W \Gamma_W} \right] \bar{u}(p_\nu, s_\nu) \\ & \times \left( -\frac{i g_W}{2\sqrt{2}} \gamma_\nu (1 - \gamma_5) \right) v(p_l, s_l), \end{aligned} \quad (2)$$

where  $\Gamma_W = 2.085 \pm 0.042$  GeV,  $m_W = 80.339$  GeV [30] and  $|V_{tb}| = 0.999152$  is the 33 entry of CKM matrix [23]. Since the term  $p_W^\mu p_W^\nu / m_W^2$  in the W-propagator is proportional to  $m_t m_l / m_W^2$  or  $m_t m_b / m_W^2$ , then it could be thrown away with good approximation. In conclusion, the Born amplitude reads

$$|M^{LO}|^2 = \frac{m_W^4 G_F^2}{2} |V_{tb}|^2 \frac{H_{\mu\nu}^{(LO)} L^{\mu\nu}}{(p_W^2 - m_W^2)^2 + m_W^2 \Gamma_W^2}, \quad (3)$$

where  $G_F = g_W^2 / (4\sqrt{2} m_W^2) = 1.16637 \times 10^{-5}$  GeV $^{-2}$  is the Fermi constant and the leptonic and hadronic tensors are

$$\begin{aligned} H_{\mu\nu}^{(LO)} = & \text{Tr}[(\not{p}_b + m_b) \gamma_\mu (1 - \gamma_5) (\not{p}_t + m_t) \\ & \times \frac{1 + \gamma_5 \not{s}_t}{2} \gamma_\nu (1 - \gamma_5)], \end{aligned} \quad (4)$$

$$L^{\mu\nu} = \text{Tr}[\not{p}_\nu \gamma^\mu (1 - \gamma_5) (\not{p}_l + m_l) \gamma^\nu (1 - \gamma_5)]. \quad (5)$$

Note that, when calculating the polarized rates from the relevant Dirac trace expressions one has to replace the completeness relations in the unpolarized Dirac string, i.e.

$\sum_{\pm 1/2} u\bar{u} = \not{p}_t + m_t$ , by the expression  $(\not{p}_t + m_t)(1 + \gamma_5 \not{s}_t)/2$ , where  $s_t$  denotes the polarization four-vector of the top quark. Using the traditional trace technique, one has

$$H_{\mu\nu}^{(LO)} L^{\mu\nu} = 128(p_b \cdot p_v)[p_t \cdot p_l - m_t(s_t \cdot p_l)], \quad (6)$$

which is independent of the bottom and lepton mass. In the top quark rest frame, the four-momentum of polarized top quark and lepton as well as the polarization four-vector of the top quark are set as

$$\begin{aligned} p_t &= (m_t; \vec{0}), \quad p_l = \frac{m_t}{2} x_l (1; \vec{0}, 1), \\ s_t &= P(0; \sin \theta_P \cos \phi, \sin \theta_P \sin \phi, \cos \theta_P), \end{aligned} \quad (7)$$

where,  $P$  is the polarization degree of top quark ( $0 \leq P \leq 1$ ) and, as was previously defined,  $x_l = 2E_l/m_t$  is the scaled energy fraction of lepton. From Fig. 1, the neutrino and b-quark four-momenta are written as

$$\begin{aligned} p_b &= \frac{m_t}{2} (1 - y^2) (1; \sin \theta_b, 0, \cos \theta_b), \\ p_v &= \frac{m_t}{2} (1 - x_l + y^2) (1; -\sin \theta_v, 0, \cos \theta_v) \end{aligned} \quad (8)$$

where  $y^2 = m_W^2/m_t^2$ ,  $\cos \theta_v = 1 - 2y^2/(x_l(1 - x_l + y^2))$  and  $\cos \theta_b = 2y^2/(x_l(1 - y^2)) - (1 + y^2)/(1 - y^2)$ . Then, for the dot product of four-momenta which are required in our calculations, one has

$$\begin{aligned} p_t \cdot p_l &= \frac{m_t^2}{2} x_l, \quad p_b \cdot p_v = \frac{m_t^2}{2} (1 - \epsilon^2 - x_l), \\ s_t \cdot p_l &= -P \frac{m_t}{2} x_l \cos \theta_P, \\ s_t \cdot p_b &= -P \frac{m_t}{2} (1 - y^2) (\cos \theta_b \cos \theta_P + \sin \theta_b \sin \theta_P \cos \phi) \end{aligned} \quad (9)$$

where we defined  $\epsilon^2 = m_b^2/m_t^2$ . By defining  $x_v = 2E_v/m_t$  and  $\gamma_W = \Gamma_W/m_W$ , the squared amplitude reads

$$\begin{aligned} |M^{LO}|^2 &= 16m_W^4 G_F^2 |V_{tb}|^2 \\ &\times \frac{x_l(1 - \epsilon^2 - x_l)}{(1 - \epsilon^2 + y^2 - x_l - x_v)^2 + y^4 \gamma_W^2} [1 + P \cos \theta_P]. \end{aligned} \quad (10)$$

Using the general definition of decay rate, the Born level rate reads

$$\begin{aligned} d\Gamma^{LO}(t \rightarrow bl^+ \nu_l) &= \frac{1}{2m_t} |M^{LO}|^2 \frac{d^3 \mathbf{p}_b}{(2\pi)^3 2E_b} \\ &\times \frac{d^3 \mathbf{p}_l}{(2\pi)^3 2E_l} \frac{d^3 \mathbf{p}_v}{(2\pi)^3 2E_v} (2\pi)^4 \delta^4(\mathbf{p}_t - \mathbf{p}_b - \mathbf{p}_l - \mathbf{p}_v). \end{aligned} \quad (11)$$

Ignoring more details, one has

$$\frac{d^3 \Gamma^{LO}}{d \cos \theta_P d\phi dx_l} = \frac{4|V_{tb}|^2 G_F^2 m_t^5}{(4\pi)^4} y^4 x_l (1 - \epsilon^2 - x_l)$$

$$\times \int \frac{dx_v}{(1 - \epsilon^2 + y^2 - x_l - x_v)^2 + y^4 \gamma_W^2} [1 + P \cos \theta_P], \quad (12)$$

where the neutrino energy ranges as:  $1 - \epsilon^2 - x_l \leq x_v \leq (1 - \epsilon^2 - x_l)/(1 - x_l)$ . By comparing Eqs. (1) and (12) one has

$$\begin{aligned} \frac{d\Gamma_A^{LO}}{dx_l} &= \frac{d\Gamma_B^{LO}}{dx_l} = 12\Gamma_F \frac{x_l(1 - \epsilon^2 - x_l)}{\gamma_W} y^2 \\ &\times \left[ \cot^{-1} \gamma_W + \cot^{-1} \frac{y^2(x_l - 1)\gamma_W}{y^2 - x_l(1 - \epsilon^2 + y^2 - x_l)} \right], \\ \frac{d\Gamma_C^{LO}}{dx_l} &= 0, \end{aligned} \quad (13)$$

where  $\Gamma_F = m_t^5 G_F^2 |V_{tb}|^2 / (192\pi^3)$  is a reference rate corresponding to a (hypothetical) point-like four-Fermion interaction. By ignoring the bottom quark mass ( $m_b = 0$ ) our results are in complete agreement with the ones in Ref. [27]. For the integrated rates (with  $m_b = 0$ ) one obtains the following analytical results

$$\begin{aligned} \Gamma_A^{LO} &= \Gamma_B^{LO} = \Gamma_F [2\pi \frac{m_W}{\Gamma_W}] y^2 (1 - y^2)^2 (1 + 2y^2), \\ \Gamma_C^{LO} &= 0. \end{aligned} \quad (14)$$

The fact that  $\Gamma_C^{LO} = 0$  means that the azimuthal correlation measurement has zero analyzing power to analyses the polarization of top quark. Non-zero contributions arise from the QCD radiative corrections. Moreover, the equality  $\Gamma_A^{LO} = \Gamma_B^{LO}$  means that the proposed polar correlation measurement has 100% analyzing power to analyze the polarization of top quark. In Refs. [31, 32], the NLO decay rates are approximated as follows

$$\begin{aligned} &\frac{d^2 \Gamma^{NLO}}{d \cos \theta_P d\phi} (t(\uparrow) \rightarrow bl^+ \nu_l) \\ &= \frac{\Gamma_A^{LO}}{4\pi} \left[ (1 - 0.0854) + P(1 - 0.0871) \cos \theta_P \right. \\ &\quad \left. + P(0 - 0.0024) \sin \theta_P \cos \phi \right], \end{aligned} \quad (15)$$

where  $\Gamma_A^{LO} = 0.1635$ . As is seen, the radiative corrections to the rate  $\Gamma_A$  and the polar correlation function  $\Gamma_B$  go in the same direction and are very close in magnitude. Moreover, the azimuthal correlation generated by the radiative corrections is still quite small. It is, then, safe to say that, if top quark decays reveal a violation of the SM (V-A) current structure in the azimuthal correlation function which exceeds the 0.3% level, the violation must have a non-SM origin. In the following, we compute the effect of Lorentz symmetry violation on the helicity components of decay rates at the Born level in the minimal SME framework. We shall show that the LV effect leads to the value for the azimuthal correlation contribution

which exceeds the 0.3% level (numerical results at LO in the minimal SME framework will be given in Eq. (28)).

### 3 Minimal SME Lagrange density for the top quark

The minimal SME is well suited for comparing the results of experimental Lorentz tests. Its generalized Lagrange density includes operators of 3 and 4 mass dimensions with their outstanding indices contracted with those of tensor-valued coefficients. A subset of CPT-even interactions on quarks from the minimal SME is [5]

$$\mathcal{L}^{\text{CPT}^+} \supset \frac{1}{2} i c_{Q_i}^{\mu\nu} \overleftrightarrow{Q}_i \gamma_\mu \overleftrightarrow{D}_\nu Q_i + \frac{1}{2} i c_{U_i}^{\mu\nu} \overleftrightarrow{U}_i \gamma_\mu \overleftrightarrow{D}_\nu U_i + \frac{1}{2} i c_{D_i}^{\mu\nu} \overleftrightarrow{D}_i \gamma_\mu \overleftrightarrow{D}_\nu D_i, \quad (16)$$

where  $D^\nu$  is the conventional gauge-covariant derivative. The conventional SM fields are denoted by

$$Q_i = \begin{pmatrix} u_i \\ d_i \end{pmatrix}_L, \quad U_i = (u_i)_R, \quad D_i = (d_i)_R, \quad (17)$$

where the label  $i (= 1, 2, 3)$  denotes the quark flavors, i.e.,  $u_i = (u, c, t)$  and  $d_i = (d, s, b)$ . The dimensionless Lorentz coefficients  $c_{Q_i}^{\mu\nu}$ ,  $c_{U_i}^{\mu\nu}$ , and  $c_{D_i}^{\mu\nu}$  remain invariant under observer Lorentz transformations and the nonzero expectation values of these tensors causes the broken under particle Lorentz transformations. In this work, we focus on the top quark decay and only assume the third generation of flavors,  $i = 3$ , dropping the index  $Q_i$ . According to the left chiral (V-A) nature of charged current in the SM, the relevant electroweak sector of the conventional SM Lagrangian for top quark decay,  $t \rightarrow b W^+ \rightarrow b l^+ \nu_l$ , is defined by

$$\mathcal{L}^{\text{SM}} \supset \frac{i}{2} \bar{t} \gamma^\mu \overleftrightarrow{\partial}_\mu t - m_t \bar{t} t + \frac{g_W V_{tb}}{\sqrt{2}} W_\mu^- \bar{b}_L \gamma^\mu t_L + (\text{h.c.}), \quad (18)$$

where  $t$  and  $\bar{t}$  are the Dirac fields for top quarks and antiquarks and  $m_t$  is the top quark mass.

The equivalence CPT-even Lorentz violating part of SME Lagrangian can be written as the following form [5,33]

$$\mathcal{L}_{\text{CPT}^+}^{\text{SME}} \supset \frac{i}{2} c_L^{\mu\nu} \bar{t}_L \gamma_\mu \overleftrightarrow{\partial}_\nu t_L + \frac{g_W V_{tb}}{\sqrt{2}} c_L^{\mu\nu} W_\nu^- \bar{b}_L \gamma_\mu t_L + (\text{h.c.}), \quad (19)$$

where the  $c_L^{\mu\nu}$  ( $\equiv c_{Q_i}^{\mu\nu}$ ) is a constant  $4 \times 4$  matrix, breaking Lorentz invariance of the Lagrangian for the left-handed part of quarks. It indicates preferential direction in space-time as seen by top quarks. The coefficient  $c_L^{\mu\nu}$  affects on the

top propagator and the  $t b W^+$ -vertex. Therefore, at LO the effect of Lorentz violation appears as an insertion in propagator and vertex. The Lorentz coefficients have the symmetric and antisymmetric parts. According to the comprehensive explanation in Ref. [33], the symmetric parts of  $c_L^{\mu\nu}$  are all physically observable and since the trace of  $c_L^{\mu\nu}$  is Lorentz invariant and can be absorbed into overall normalizations of the fields, so they can be set to zero without loss of generality. In summary, the coefficient  $c_L^{\mu\nu}$  is considered as a real, constant, dimensionless and traceless matrix. This feature has been taken into account in the following calculations for the top quark decay rates.

### 4 Angular distribution of decay rate in the minimal SME theory

If we just preserve the coefficient  $c_L^{\mu\nu}$  ( $\mu = T, X, Y, Z$ ) in the minimal SME Lagrangian as the LV coefficient, Eq. (19), the corrections arising via vertex and propagator insertions can be written as

$$\gamma^\mu \rightarrow \gamma^\mu + c_L^{\mu\nu} \gamma_\nu, \quad \not{p}_t + m_t \rightarrow (\not{p}_t + \tilde{m}_t), \quad (20)$$

where, following Ref. [34] we have introduced the convenient notation:  $\tilde{m}_t = m_t(1 - c_L^{00})$ . Moreover, the Metric tensor reads:  $\tilde{g}^{\mu\nu} = g^{\mu\nu} + C_L^{\mu\nu}$  where  $C_L^{\mu\nu} = c_L^{\mu\nu} - c_L^{\mu 0} g^{\nu 0} + c_L^{\nu 0} g^{\mu 0} - c_L^{00} g^{\mu\nu}$ . This leads to  $\not{p}_t = \tilde{g}_{\mu\nu} \gamma^\mu \not{p}_t^\nu = \not{p}_t(1 - (c_L)_{00}) + (c_L)_{\mu\nu} \gamma^\mu \not{p}_t^\nu - (c_L)_{\mu 0} \gamma^\mu \not{p}_t^0 + (c_L)_{\nu 0} \gamma^0 \not{p}_t^\nu$ . Therefore, the following replacement should be considered

$$(\not{p}_t + m_t) \rightarrow (\not{p}_t + m_t)(1 - (c_L)_{00}) + (c_L)_{\mu\nu} \gamma^\mu \not{p}_t^\nu - m_t (c_L)_{\mu 0} \gamma^\mu + (c_L)_{\nu 0} \gamma^0 \not{p}_t^\nu. \quad (21)$$

These quantities have nontrivial Lorentz-transformation properties. By replacing these corrections into Eq. (4), the hadronic tensor reads:  $H_{\mu\nu} = H_{\mu\nu}^{LO} + H_{\mu\nu}^{LV}$ , in which the first term is the Lorentz-invariant SM hadronic tensor given in Eq. (4) and the new term represents the correction arising at leading order in the  $c_L^{\mu\nu}$  coefficient. It reads

$$H_{\mu\nu} = \text{Tr}[(\not{p}_b + m_b)(\gamma_\mu + (c_L)_{\mu\alpha} \gamma^\alpha)(1 - \gamma_5)(\not{p}_t + \tilde{m}_t) \times \frac{1 + \gamma_5 \not{s}_t}{2} (\gamma_\nu + (c_L)_{\nu\beta} \gamma^\beta)(1 - \gamma_5)]. \quad (22)$$

The leptonic tensor (Eq. (5)) remains unchanged. To compute the polarized and unpolarized decay rates we use the same technique described in Sect. 2. The four-momentum dot products are given in Eq. (9). Keeping only linear terms in  $c^{\mu\nu}$ , the unpolarized differential decay rate is obtained as

$$\frac{d\Gamma_A^{LV}}{dx_l} = \frac{3y^2 \Gamma_F}{8\gamma_W} \left[ \cot^{-1} \gamma_W + \cot^{-1} \frac{y^2 \gamma_W}{x_l - y^2} \right]$$

$$\begin{aligned} & \times \left\{ 32(1-x_l)[x_l(1-c_L^{ZZ}) + (x_l-y^2)c_L^{TT} \right. \\ & + y^2(c_L^{XX} + c_L^{YY} + 3c_L^{ZZ})] \\ & - 32y[x_l c_L^{TX} + (x_l-2)c_L^{XZ}] \\ & \left. \times \sqrt{(1-x_l)(x_l-y^2)} \right\}. \end{aligned} \quad (23)$$

For the polar differential decay rate, one has

$$\begin{aligned} \frac{d\Gamma_B^{LV}}{dx_l} = & \frac{12y^2\Gamma_F}{\gamma_W} \left[ \cot^{-1}\gamma_W + \cot^{-1}\frac{y^2\gamma_W}{x_l-y^2} \right] \\ & \times \left\{ (1-x_l)[x_l(1-c_L^{ZZ}) - y^2(c_L^{TT} \right. \\ & - c_L^{XX} - c_L^{YY} - 3c_L^{ZZ})] \\ & \left. - y[x_l c_L^{TX} + (x_l-2)c_L^{XZ}] \sqrt{(1-x_l)(x_l-y^2)} \right\}. \end{aligned} \quad (24)$$

Finally the azimuthal differential decay rate, which has zero contribution in the SM, reads

$$\begin{aligned} \frac{d\Gamma_C^{LV}}{dx_l} = & \frac{12y^2\Gamma_F}{\gamma_W} \left[ \cot^{-1}\gamma_W + \cot^{-1}\frac{y^2\gamma_W}{x_l-y^2} \right] \\ & \times \left\{ (2y^2-x_l)(1-x_l)(c_L^{TX} + c_L^{XZ}) \right. \\ & + y[(x_l-1)(c_L^{TT} + 2c_L^{TZ}) + c_L^{YY} \\ & \left. + 3c_L^{XX} + (1+x_l)c_L^{ZZ}] \sqrt{(1-x_l)(x_l-y^2)} \right\}. \end{aligned} \quad (25)$$

If one sets  $c_L^{\mu\nu} = 0$ , the SM results are restored. These analytical results are presented for the first time and could be applied to study the LV effect on the top quark decay at the CERN-LHC and future high energy colliders.

## 5 Reference frames: laboratory and Sun-centered frames

In previous section we obtained the analytical results (23–25) for the unpolarized, polar and azimuthal rates in the rest frame of top quark through the theories of SM and SME. Results in the SM are independent of the chosen frame while the SME rates are related to the LV coefficients which are frame-dependent. For our purpose, we take these coefficients from Ref. [35] reported by the CERN-CMS Collaboration. In their work, to report the measurements of LV coefficients the sun-centered frame (SCF), as the theoretical setup, is employed. It is physically reasonable to take the LV coefficients as constants in the SCF [36]. The SCF is defined so as its origin is located at the center of the sun and the Z-axis of its Cartesian coordinates ( $T$ ,  $X$ ,  $Y$ ,  $Z$ ) is pointed to north

parallel to the earth's rotation axis, its X-axis is pointed to the intersection of the ecliptic and celestial equator on January 1st, 2000(J2000), and the Y-axis completes the direct basis [37]. The SCF can be considered as inertial in the life time of a physics experiment. The relevant measure of time in such a reference frame is called sidereal time. While one rotation period of the earth is equal to approximately 23 h 56 min UTC, it is defined as being equal to 24 sidereal hours. In Ref. [35] it is pointed out that the CMS data is recorded in UNIX time which is identical to standard UTC time for their considered purpose. The UNIX timestamp of the events is translated to sidereal time with the formula (2) in Ref. [35].

The CMS detector is moving around the earth's rotation axis during a sidereal day, and so does the beam line direction at the interaction point, or the average direction of top quarks produced in the collisions. As a consequence, top quark couplings with  $c_{\mu\nu}$  depend on time, resulting in cross sections for top production modulating with sidereal time.

Within the CMS reference frame, the variation of the  $t\bar{t}$  cross section with sidereal time  $t$  is quantified with the function  $f(t) = \sigma_{SME}(t)/\sigma_{SM} - 1$ , where  $\sigma_{SME}(\sigma_{SM})$  are the cross sections predicted in the SME (SM), see Eq. (3) in Ref. [35]. The function  $f(t)$  depends on the Rotation matrices  $R$  which represent transformations of observer coordinates from the SCF to the CMS reference frame, depending on the earth's rotation around its axis with angular velocity  $\omega_{\oplus}$  sidereal (boosts associated with this rotation and with the revolution around the sun are negligible relative to top quark boosts). The transformation between the SCF and a laboratory frame is comparatively simple. Suppose, for example, that Cartesian coordinates ( $t$ ,  $x$ ,  $y$ ,  $z$ ) in the laboratory are chosen such that the x-axis points south, the y-axis points east, and the z-axis points vertically upwards. Since the Earth rotates with sidereal frequency  $\omega_{\oplus}$  the relationship mapping coefficients in the laboratory frame to those in the SCF involves a time-dependent rotation  $R^{Jj}$  between the two coordinate systems [38]. With the reasonable approximation that the orbit of the Earth is circular, the rotation from the Sun-centered celestial equatorial frame to the standard laboratory frame is given by

$$R^{Jj} = \begin{bmatrix} \cos\chi \cos\omega_{\oplus}T \cos\chi \sin\omega_{\oplus}T - \sin\chi & \\ -\sin\omega_{\oplus}T & \cos\omega_{\oplus}T & 0 \\ \sin\chi \cos\omega_{\oplus}T \sin\chi \sin\omega_{\oplus}T & \cos\chi \end{bmatrix} \quad (26)$$

where  $\chi$  is the colatitude of experiment/laboratory (in a spherical coordinate system, a colatitude is the complementary angle of a given latitude). Moreover,  $j = x, y, z = 1, 2, 3$  denotes an index in the laboratory frame, while  $J = X, Y, Z$  denotes an index in the SCF. The time  $T$  is measured in the SCF from one of the times when the  $y$ - and  $Y$ -axes coincide, to be chosen conveniently for each experiment. Since the coefficients in the laboratory frame can be obtained from those in the SCF via the above rotation, exper-

imental results can readily be reported directly in terms of coefficients in the SCF. Since the transformation to the laboratory frame involves the time-dependent rotation, the laboratory frame coefficients vary with sidereal time.

The coordinates of CMS interaction point are specified by the azimuth on the LHC ring ( $\phi = 101.28^\circ$ ), the latitude ( $\lambda = 46.31^\circ N$ ), and the longitude ( $l = 6.08^\circ E$ ). Furthermore the LHC plane, and thus the CMS cavern, has an angle of  $\alpha = 0.705^\circ$  relative to the surface (geodetic plane). In Ref. [35], it is described that the signal  $f(\mathbf{t})$  functions are computed as a function of the number of reconstructed  $b$  jets separately for each year and sidereal time bin.

It should be noted that, due to very short lifetime of top quark ( $\tau \approx 0.5 \times 10^{-24}$  s) the effect of transformations between the SCF and the TRF is similar to the one between the SCF and the CMS laboratory frame. In fact, according to the uncertainty relation  $\Delta E \Delta t \approx \hbar$  one has  $\Delta E \approx 0.6$  GeV which leads to the Lorentz factor:  $\gamma = 1/\sqrt{1 - \beta^2} \approx 1.003$ . This value is corresponding to the relative speed of TRF and CMS frame much less than the speed of light  $v_{rel} \approx 0.057c$ . In this nonrelativistic limit ( $v_{rel}/c \ll 1$ ), the Lorentz transformation matrix between the TRF and CMS frame is  $\Lambda \approx \mathbb{1}$ .

## 6 Numerical analysis

In the analytical results obtained for the differential decay rates, the LV (or the SME Wilson) coefficients appear as the combinations of  $c_L^{TX}$ ,  $c_L^{TZ}$ ,  $c_L^{XZ}$  and  $c_L^{\mu\mu}$  ( $\mu = T, X, Y, Z$ ), see Eqs. (23)–(25). As was mentioned, we take these coefficients from Ref. [35] reported by the CERN-CMS Collaboration. Authors in [35] have reported a first search for the violation of Lorentz invariance in top quark pair production in proton–proton collisions ( $pp \rightarrow t\bar{t}$ ) at the LHC, at a center-of-mass energy of  $\sqrt{s} = 13$  TeV. Through their work, the Lorentz-violating coefficients  $c^{\mu\nu}$ , impacting top quarks, have been measured from events containing one electron and one muon of opposite charge in the final state ( $t\bar{t} \rightarrow b\bar{b}\mu\nu_\mu e\nu_e$ ) collected with the CMS detector. As they assert, this study is the most precise test of Lorentz invariance using top quarks at a hadron Collider.

Within the chosen basis of Wilson coefficients adopted in the SME, the matrix  $c^{\mu\nu}$  has been defined as symmetric and traceless. They have explained that, since the SME coefficients with indices  $\mu\nu = TT$  induce a shift on the  $t\bar{t}$  cross section then these coefficients are not considered. Furthermore, since the  $\hat{Z}$ -axis is defined as the earth's rotation axis and because modulation of the  $t\bar{t}$  cross section with sidereal time is induced by rotation around this axis, then there is by definition no sensitivity in the coefficients with indices  $\mu\nu = ZZ$  and  $\mu\nu = ZT$ . They have also expressed that the coefficients with  $\mu\nu = XT$  or  $\mu\nu = YT$  are found to

induce very small SME corrections and are also not considered. Remaining coefficients correspond to the combinations  $c_L^{XX} = -c_L^{YY}$ ,  $c_L^{XZ} = c_L^{ZX}$ ,  $c_L^{YZ} = c_L^{ZY}$ , and  $c_L^{XY} = c_L^{YX}$ . The measured values for the SME coefficients (in  $10^{-3}$  units) are reported as [35]

$$\begin{aligned} -1.85 &\leq c_L^{XX} \leq 2.55, & -4.36 &\leq c_L^{XY} \leq 0.07, \\ -1.15 &\leq c_L^{XZ} \leq 13.48, & -11.31 &\leq c_L^{YZ} \leq 3.24 \end{aligned} \quad (27)$$

To present our numerical results, following Ref. [35] we also assume  $c_L^{XX} = -c_L^{YY}$ ,  $c_L^{TT} = c_L^{TX} = c_L^{ZZ} = 0$ . Taking  $c_L^{XZ} = 13.48 \times 10^{-3}$  and  $c_L^{XX} = -c_L^{YY} = 2.55 \times 10^{-3}$ , for the LO integrated rates we obtain

$$\begin{aligned} \frac{d^2\Gamma^{(LO,LV)}}{d\cos\theta_p d\phi} &= \frac{\Gamma_A^{(LO,LV)}}{4\pi} \left[ 1 + P(0.9417) \cos\theta_p \right. \\ &\quad \left. + P(-0.0053) \sin\theta_p \cos\phi \right], \end{aligned} \quad (28)$$

where  $\Gamma_A^{(LO,LV)} = 0.1659$  (note that:  $\Gamma_A^{(LO,SM)} = 0.1635$ ). As is seen, the LV effect leads to a non-zero contribution for the azimuthal correlation which is around two times bigger than the NLO radiative corrections in the SM, see Eq. (15). Moreover, unlike the SM prediction for which one has  $\Gamma_A^{LO} = \Gamma_B^{LO}$ , here one has  $\Gamma_B^{(LO,LV)} = 0.9417 \Gamma_A^{(LO,LV)}$ .

Having the analytical result for  $d\Gamma_C^{LV}/dx_l$  (25) it would also be possible to determine an upper bound on the LV coefficients. To this aim, following Ref. [35] we assume  $c_L^{T\mu} = 0$  ( $\mu = T, X, Y, Z$ ) and since, the matrix  $c_L^{\mu\nu}$  is defined as symmetric and traceless then we also assume  $c_L^{ii} = 0$  ( $i = X, Y, Z$ ). Then, if we take  $\Gamma_C^{(LO,LV)} = \Gamma_C^{(NLO,SM)}$  we obtain:  $c_L^{XZ} \leq 23.6 \times 10^{-3}$  which is about two times bigger than the value reported in Eq. (27) (the value of  $\Gamma_C^{(NLO,SM)}$  is given in Eq. (15)). If we take  $c_L^{XZ} = 13.48 \times 10^{-3}$  from the values given in Eq. (27) and resolve the Eq. (25) we obtain  $c_L^{XX} \leq 2.65 \times 10^{-3}$  which is comparable with the one reported by the CMS Collaboration, see Eq. (27).

Taking the  $c_L$  values in Eq. (27) and related assumptions, in Figs. 2 and 3 the polarized and unpolarized differential decay rates, i.e.  $d\Gamma_B/dx_l$  and  $d\Gamma_A/dx_l$ , are plotted as a function of  $x_l = 2E_l/m_t$  and compared with the SM ones. In both plots, the uncertainty bands due to variation of  $c_L^{XZ}$  are also plotted. It is observed that the LV correction leads to an enhancement of the partial decay widths in the peak region by as much as (1.5–2)%.

In Fig. 4, we studied the azimuthal differential decay rate  $d\Gamma_C^{LV}/dx_l$  at LO in the LV frame. For this study, we also considered the uncertainty band due to variation of LV coefficients  $c_L^{\mu\nu}$  given in Eq. (27). As is seen, the LV effect leads to different result for the azimuthal correlation contribution which is considerable (this contribution is zero at LO in the SM). This deviation from the corresponding SM value could be considered as a situation to search for new physics. To

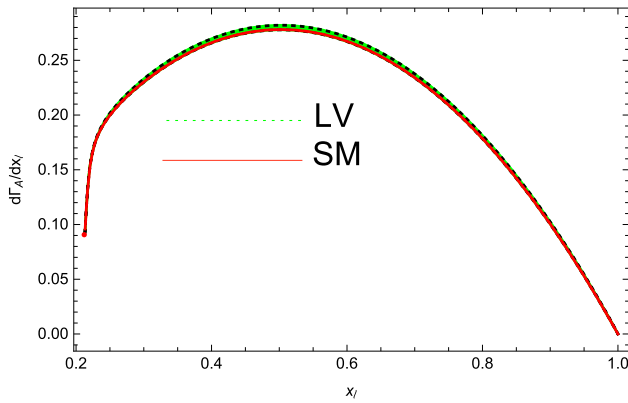


**Fig. 2** Unpolarized differential decay rate  $d\Gamma_A/dx_l$  as a function of  $x_l = 2E_l/m_t$  at LO, assuming  $c_L^{T\mu} = 0$ ,  $c_L^{ZZ} = 0$  and  $c_L^{XX} = -c_L^{YY}$ . Following Ref. [35], we take  $-1.15 \times 10^{-3} \leq c_L^{XZ} \leq 13.48 \times 10^{-3}$ . The LV decay rate (green dashed line) is compared to the SM one (red solid line)

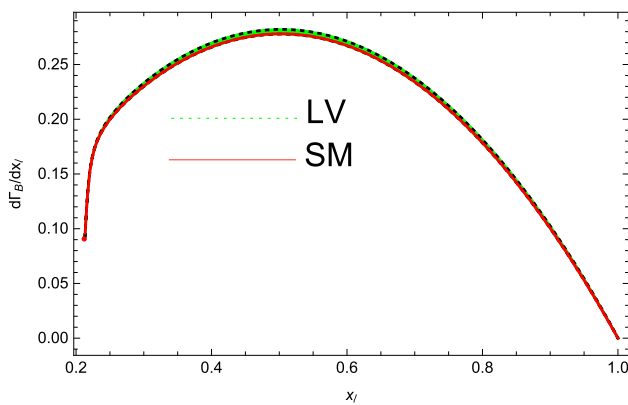


**Fig. 3** As in Fig. 2 but for the polarized contribution, i.e.  $d\Gamma_B/dx_l$ . The LV decay rate (green dashed line) is compared to the SM one (red solid line)

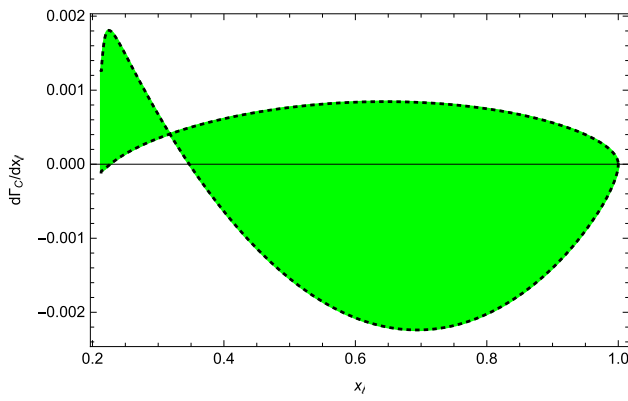


**Fig. 4** As in Fig. 2 but for the azimuthal contribution, i.e.  $d\Gamma_C^{LV}/dx_l$ . The corresponding SM value is zero. The uncertainty band due to variation of  $c_L^{XZ}$  is plotted, i.e.,  $-1.15 \times 10^{-3} \leq c_L^{XZ} \leq 13.48 \times 10^{-3}$

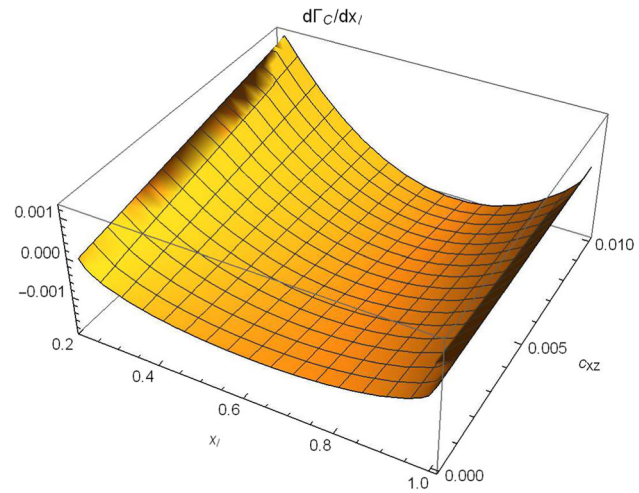


**Fig. 5** The LV azimuthal decay rate  $d\Gamma_C/dx_l$  as the functions of  $x_l$  ( $0 \leq x_l \leq 1$ ) and  $c_L^{XZ}$  ( $10^{-4} \leq c_L^{XZ} \leq 10^{-2}$ ), while we set  $c_L^{TT} = c_L^{TX} = c_L^{ZZ} = 0$  and  $c_L^{YY} = -c_L^{XX} = 2.55 \times 10^{-3}$

have a more detail insight on effect of LV coefficients on the azimuthal contribution, in Fig. 5 we plotted the azimuthal differential decay rate  $d\Gamma_C/dx_l$  as the functions of  $x_l$  ( $0 \leq x_l \leq 1$ ) and  $c_L^{XZ}$  ( $10^{-4} \leq c_L^{XZ} \leq 10^{-2}$ ). Here, following the CMS assumption we set  $c_L^{TT} = c_L^{TX} = c_L^{ZZ} = 0$  and  $c_L^{YY} = -c_L^{XX}$  and took the upper value of  $c_L^{XX} = 2.55 \times 10^{-3}$ . As is seen, the bigger values of  $c_L^{XZ}$  have more effect on the differential decay rate at large and small regions of  $x_l$  (at  $x_l \approx 0.2$  and  $x_l \approx 1$ ), while for the middle regions of  $x_l$  ( $0.4 < x_l < 0.8$ ) the sensitivity of decay rate to the variation of  $c_L^{XZ}$  is less. In Fig. 6, the same study is done but for the lower limit of  $c_L^{XX}$  as  $c_L^{XX} = -1.85 \times 10^{-3}$ . As is observed, this leads to a different result for the  $d\Gamma_c/dx_l$  so that for smaller values of  $c_L^{XZ}$  the behavior of differential decay rate is completely different with the one in Fig. 5. For bigger values of  $c_L^{XZ}$ , i.e.,  $5 \times 10^{-3} \leq c_L^{XZ} \leq 10^{-2}$ , the behavior of  $d\Gamma_c/dx_l$  is the same as in Fig. 5.

In Fig. 7, the LV azimuthal differential decay rate is shown as the functions of  $c_L^{XX}$  ( $10^{-4} \leq c_L^{XX} \leq 10^{-2}$ ) and  $c_L^{XZ}$  ( $10^{-4} \leq c_L^{XZ} \leq 10^{-2}$ ) for  $x_l = 0.7$  (the position of second peak in Fig. 4) and in Fig. 8, the same plot is shown for  $x_l = 0.225$  (first peak position in Fig. 4). As is seen, at  $x_l = 0.225$  the effect of  $c_L^{XZ}$ -coefficient on the differential decay rate is more important than the  $c_L^{XX}$  while at  $x_l = 0.7$  the variation effect of  $c_L^{XX}$  is more effective.

## 7 Conclusions

Since the top quark decays before hadronization takes place, then it offers a unique arena for studying Lorentz symmetry in essentially free quarks. In the present work, we explored the prospects for studying the foundational Lorentz symme-

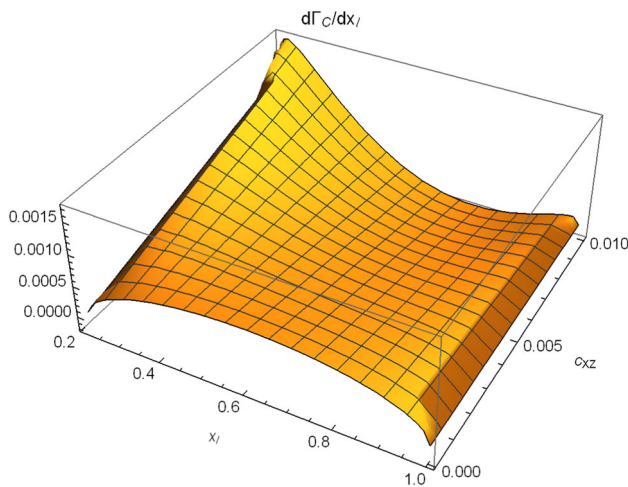


**Fig. 6** As in Fig. 5 but for  $c_L^{XX} = -1.85 \times 10^{-3}$

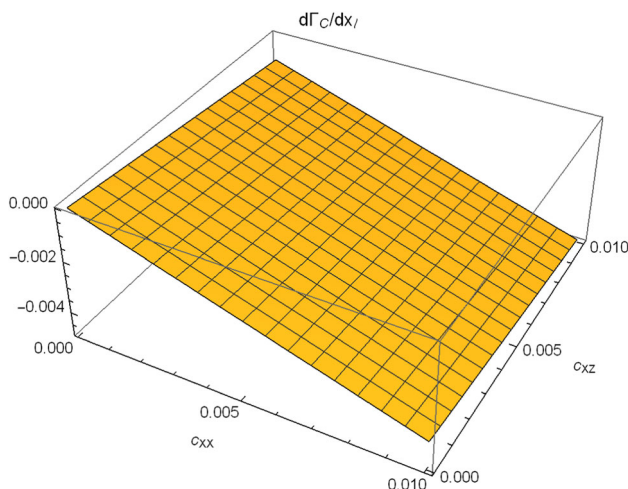


**Fig. 7** The azimuthal decay rate  $d\Gamma_C/dx_l$  at the LV framework as the functions of  $c_L^{XX}$  ( $10^{-4} \leq c_L^{XX} \leq 10^{-2}$ ) and  $c_L^{XZ}$  ( $10^{-4} \leq c_L^{XZ} \leq 10^{-2}$ ) for  $x_l = 0.7$  (second peak position in Fig. 4). Here, we set  $c_L^{TT} = c_L^{TX} = c_L^{ZZ} = 0$  and  $c_L^{YY} = -c_L^{XX}$

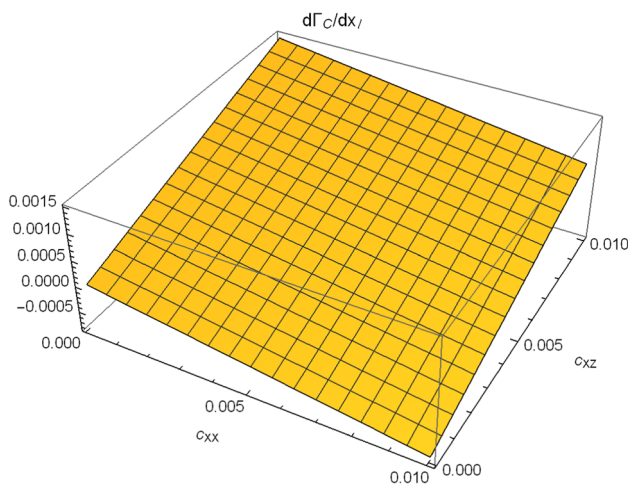


**Fig. 8** As in Fig. 7 but for  $x_l = 0.225$  (first peak position in Fig. 4)

try of the SM at the scale of top quark. Therefore we studied the effect of LV on the angular distributions of polarized top quark decay rate in the minimal SME framework. Our results showed that, unlike the prediction of SM, within the SME framework one has  $\Gamma_B^{(LO,LV)} \neq \Gamma_A^{(LO,LV)}$  where  $\Gamma_A$  and  $\Gamma_B$  are the unpolarized and the polarized decay rates. Using the analytical results, which are presented for the first time, we also determined an upper bound on the LV coefficients as  $c_L^{XZ} \leq 23.6 \times 10^{-3}$  and  $c_L^{XX} \leq 2.65 \times 10^{-3}$  which are in good consistency with the values reported by the CMS Collaboration. Using the values of LV coefficients reported by the CMS Collaboration we showed that the azimuthal correlation, which is absent in the SM at lowest order perturbation theory, is about two times bigger than the NLO radiative corrections in the SM. This could be a new channel to test the Lorentz violation effect at the LHC. Although, the azimuthal decay rate is small, but it may then be feasible to experimentally measure the azimuthal correlations produced through top decays in future high energy colliders. Highly polarized top quarks will become available in singly produced top quarks at hadron colliders (see e.g. [26]) and in top quark pairs produced in future linear  $e^+e^-$  colliders [25, 39].

It should be noted that, our analysis is based on the results presented by the CMS Collaboration [35] where to extract the LV coefficients the sun-centered frame, as the theoretical setup, is employed. Therefore, our analysis is valid in the same reference frame. Since the coefficients in the laboratory frame can be obtained from those in the SCF via the rotation matrix (26), then experimental results can readily be reported directly in terms of coefficients in the SCF.

Another point: Signals of Lorentz violation have unique features that cannot be associated with Lorentz-invariant effects. For example, in a given inertial frame, the presence of Lorentz violation means that the properties of each quark depend on its direction of travel and its boost. These features lead to distinctive experimental signals that provide a basis for searches for Lorentz violation in the top-quark sector. Since the transformation to the laboratory frame involves the time-dependent rotation (Eq. (26)), then the laboratory frame coefficients vary with sidereal time while the LV coefficients are constant in the Sun-centered frame. Lorentz violation, therefore, can be expected to produce sidereal oscillations in the data, with amplitudes and phases governed by the coefficients for Lorentz violation. Most coefficients produce signals at the sidereal frequency  $\omega_{\oplus}$ , but the symmetric components of the coefficient  $c_{\mu\nu}$  generate ones at the harmonic  $2\omega_{\oplus}$  as well [33]. Then, the data for top quark decay can be expected to contain information in the amplitudes and phases of the sidereal and twice-sidereal harmonics (see, for example, Fig. 3 in Ref. [35] where the  $t\bar{t}$  normalized differential

cross section is shown as a function of sidereal time, using combined 2016 and 2017 data).

**Funding** There is no funding for our work.

**Data Availability Statement** This manuscript has no associated data. [Author's comment: The needed input parameters can be found in the text and references of this paper.]

**Code Availability Statement** This manuscript has no associated code/software. [Author's comment: All required information on the CODE/SOFTWARE applied is given in the manuscript.]

**Open Access** This article is licensed under a Creative Commons Attribution 4.0 International License, which permits use, sharing, adaptation, distribution and reproduction in any medium or format, as long as you give appropriate credit to the original author(s) and the source, provide a link to the Creative Commons licence, and indicate if changes were made. The images or other third party material in this article are included in the article's Creative Commons licence, unless indicated otherwise in a credit line to the material. If material is not included in the article's Creative Commons licence and your intended use is not permitted by statutory regulation or exceeds the permitted use, you will need to obtain permission directly from the copyright holder. To view a copy of this licence, visit <http://creativecommons.org/licenses/by/4.0/>.

Funded by SCOAP<sup>3</sup>.

## References

1. V.A. Kostelecky, R. Potting, CPT, strings, and meson factories. *Phys. Rev. D* **51**, 3923–3935 (1995)
2. V.A. Kostelecky, R. Potting, CPT and strings. *Nucl. Phys. B* **359**, 545–570 (1991)
3. P. Horava, Quantum gravity at a Lifshitz point. *Phys. Rev. D* **79**, 084008 (2009)
4. D. Colladay, V.A. Kostelecky, CPT violation and the standard model. *Phys. Rev. D* **55**, 6760–6774 (1997)
5. D. Colladay, V.A. Kostelecky, Lorentz violating extension of the standard model. *Phys. Rev. D* **58**, 116002 (1998)
6. J.D. Tasson, What do we know about Lorentz invariance? *Rep. Prog. Phys.* **77**, 062901 (2014)
7. R. Bluhm, Overview of the SME: implications and phenomenology of Lorentz violation. *Lect. Notes Phys.* **702**, 191–226 (2006)
8. V. Ekraminasab, S.M. Moosavi Nejad, Study of Lorentz violation in hadron production process from pair annihilation induced by a nonminimal coupling. *Eur. Phys. J. C* **84**(4), 430 (2024)
9. B. Charneski, M. Gomes, R.V. Maluf, A.J. da Silva, Lorentz violation bounds on Bhabha scattering. *Phys. Rev. D* **86**, 045003 (2012)
10. H. Belich, T. Costa-Soares, M.M. Ferreira Jr., J.A. Helayel-Neto, F.M.O. Moucherek, Lorentz-violating corrections on the hydrogen spectrum induced by a non-minimal coupling. *Phys. Rev. D* **74**, 065009 (2006)
11. V.A. Kostelecky, C.D. Lane, Constraints on Lorentz violation from clock comparison experiments. *Phys. Rev. D* **60**, 116010 (1999)
12. R. Bluhm, V.A. Kostelecky, C.D. Lane, CPT and Lorentz tests with muons. *Phys. Rev. Lett.* **84**, 1098–1101 (2000)
13. R. Bluhm, V.A. Kostelecky, N. Russell, CPT and Lorentz tests in hydrogen and anti-hydrogen. *Phys. Rev. Lett.* **82**, 2254–2257 (1999)
14. D. Mattingly, Modern tests of Lorentz invariance. *Living Rev. Relativ.* **8**, 5 (2005)
15. R.M. Barnett et al., [Particle Data Group], Review of particle physics. *Particle Data Group. Phys. Rev. D* **54**(1), 1–720 (1996)
16. B. Schwingenheuer, R.A. Briere, A.R. Barker, E. Cheu, L.K. Gibbons, D.A. Harris, G. Makoff, K.S. McFarland, A. Roodman, Y.W. Wah et al., CPT tests in the neutral kaon system. *Phys. Rev. Lett.* **74**, 4376–4379 (1995)
17. R. Carosi et al., [NA31], A measurement of the phases of the CP violating amplitudes in  $K^0 \rightarrow 2\pi$  decays and a test of CPT invariance. *Phys. Lett. B* **237**, 303–312 (1990)
18. J.M. Brown, S.J. Smullin, T.W. Kornack, M.V. Romalis, New limit on Lorentz and CPT-violating neutron spin interactions. *Phys. Rev. Lett.* **105**, 151604 (2010)
19. S. Abachi et al., [D0], Search for high mass top quark production in  $p\bar{p}$  collisions at  $\sqrt{s} = 1.8$  TeV. *Phys. Rev. Lett.* **74**, 2422–2426 (1995)
20. V.A. Kostelecky, Gravity, Lorentz violation, and the standard model. *Phys. Rev. D* **69**, 105009 (2004)
21. R. Bluhm, Explicit versus spontaneous diffeomorphism breaking in gravity. *Phys. Rev. D* **91**(6), 065034 (2015)
22. K.G. Chetyrkin, R. Harlander, T. Seidensticker, M. Steinhauser, Second order QCD corrections to  $\Gamma(t \rightarrow W b)$ . *Phys. Rev. D* **60**, 114015 (1999)
23. N. Cabibbo, Unitary symmetry and leptonic decays. *Phys. Rev. Lett.* **10**, 531 (1963)
24. M. Kobayashi, T. Maskawa, CP violation in the renormalizable theory of weak interaction. *Prog. Theor. Phys.* **49**, 652 (1973)
25. S.J. Parke, Y. Shadmi, Spin correlations in top quark pair production at  $e^+e^-$  colliders. *Phys. Lett. B* **387**, 199–206 (1996)
26. G. Mahlon, S.J. Parke, Improved spin basis for angular correlation studies in single top quark production at the Tevatron. *Phys. Rev. D* **55**, 7249 (1997)
27. S. Groote, W.S. Huo, A. Kadeer, J.G. Korner, Azimuthal correlation between the (vector- $p(\ell)$ , vector- $p(X(b))$ ) and (vector- $p(\ell)$ , vector- $P(t)$ ) planes in the semileptonic rest frame decay of a polarized top quark: an  $O(\alpha(s))$  effect. *Phys. Rev. D* **76**, 014012 (2007)
28. M. Fischer, S. Groote, J.G. Körner, M.C. Mauser, B. Lampe, Polarized top decay into polarized  $W: t(\text{polarized}) \rightarrow W(\text{polarized}) + b$  at  $O(\alpha(s))$ . *Phys. Lett. B* **451**, 406 (1999)
29. S.M. Moosavi Nejad, S. Abbaspour, R. Farashahian, Interference effects for the top quark decays  $t \rightarrow b + W^+ / H^+ (\rightarrow \tau^+ \nu_\tau)$ . *Phys. Rev. D* **99**(9), 095012 (2019)
30. K. Nakamura et al., (Particle Data Group), Review of particle physics. *J. Phys. G* **37**, 075021 (2010)
31. A. Czarnecki, M. Jezabek, Distributions of leptons in decays of polarized heavy quarks. *Nucl. Phys. B* **427**, 3–21 (1994)
32. M. Fischer, S. Groote, J.G. Körner, M.C. Mauser, Complete angular analysis of polarized top decay at  $O(\alpha(s))$ . *Phys. Rev. D* **65**, 054036 (2002)
33. M.S. Berger, V.A. Kostelecký, Z. Liu, Lorentz and CPT violation in top-quark production and decay. *Phys. Rev. D* **93**(3), 036005 (2016)
34. D. Colladay, V.A. Kostelecky, Cross-sections and Lorentz violation. *Phys. Lett. B* **511**, 209–217 (2001)
35. [CMS], Searches for violation of Lorentz invariance in  $t\bar{t}$  production using dilepton events in proton–proton collisions at  $\sqrt{s} = 13$  TeV. CMS-PAS-TOP-22-007
36. V.A. Kostelecky, Sensitivity of CPT tests with neutral mesons. *Phys. Rev. Lett.* **80**, 1818 (1998)
37. J. Kamoshita, Probing noncommutative space-time in the laboratory frame. *Eur. Phys. J. C* **52**, 451–457 (2007)
38. V.A. Kostelecky, M. Mewes, Signals for Lorentz violation in electrodynamics. *Phys. Rev. D* **66**, 056005 (2002)
39. J.H. Kuhn, How to measure the polarization of top quarks. *Nucl. Phys. B* **237**, 77–85 (1984)